ANTIOXIDANTS & REDOX SIGNALING
Volume 13, Number 5, 2010

DOI: 10.1089/ars.2009.2976

ORIGINAL RESEARCH COMMUNICATION

Dysfunction of Glutathione S-Transferase Leads to Excess 4-Hydroxy-2-Nonenal and H_2O_2 and Impaired Cytokine Pattern in Cultured Keratinocytes and Blood of Vitiligo Patients

Vladimir A. Kostyuk,[1,2] Alla I. Potapovich,[1,2] Eleonora Cesareo,[1] Serena Brescia,[1] Liliana Guerra,[1] Giuseppe Valacchi,[3,4] Alessandra Pecorelli,[3] Irina B. Deeva,[1,5] Desanka Raskovic,[6] Chiara De Luca,[1] Saveria Pastore,[1] and Liudmila G. Korkina[1]

Abstract

Oxidative stress due to increased epidermal levels of H_2O_2 with consequent inhibition of catalase activity is generally accepted as a leading cytotoxic mechanism of melanocyte loss in vitiligo. Keratinocyte-derived cytokines are considered key factors in the maintenance of melanocyte structure and functions. We hypothesized that abnormal redox control may lead to impaired cytokine production by keratinocytes, thus causing noncytotoxic defects in melanocyte proliferation and melanogenesis. We found significantly suppressed mRNA and protein expression of glutathione-S-transferase (GST) M1 isoform, and higher-than-normal levels of both 4-hydroxy-2-nonenal (HNE)-protein adducts and H_2O_2 in the cultures of keratinocytes derived from unaffected and affected skin of vitiligo patients, and in their co-cultures with allogeneic melanocytes. GST and catalase activities, as well as glutathione levels, were dramatically low in erythrocytes, whilst HNE–protein adducts were high in the plasma of vitiligo patients. The broad spectrum of major cytokines, chemokines, and growth factors was dysregulated in both blood plasma and cultured keratinocytes of vitiligo patients, when compared to normal subjects. Exogenous HNE added to normal keratinocytes induced a vitiligo-like cytokine pattern, and H_2O_2 overproduction accompanied by adaptive upregulation of catalase and GSTM1 genes, and transient inhibition of Erk1/2 and Akt phosphorylation. Based on these results, we suggest a novel GST-HNE-H_2O_2-based mechanism of dysregulation of cytokine-mediated keratinocyte–melanocyte interaction in vitiligo. *Antioxid. Redox Signal.* 13, 607–620.

Introduction

VITILIGO IS A COMMON SKIN DISEASE recognized hundreds of years ago, characterized by the appearance of depigmented areas. Nonetheless, its etiology, as well as the pathogenic mechanisms underlying melanin-producing cell loss [vitiligo "puzzle" (43)], still remain unclear. The disease has a complex nature, with both genetically transmitted and acquired factors. Vitiligo has long been considered an oxidative stress-related pathology, because of the evident imbalance between reactive oxygen species (ROS) production and neutralization, and the presence of oxidative stress lipid and protein markers in the skin and circulating blood (12, 13, 35, 46). Owing to the intense research by Schallreuter's group (35, 36), the loss of active melanocytes is commonly considered a result of H_2O_2 cytotoxicity. As major sources of H_2O_2 overproduction in vitiligo epidermis, NADPH oxidase (NOX) of keratinocytes and fibroblasts, estrogen, catechol, and catecholamine metabolisms have been suggested (36, 43). Further support to the cytotoxic hypothesis has been provided by data on the increased levels of ROS in the circulating white blood cells of vitiligo patients (13). This feature was attributed to impaired mitochondrial functions, consequent to the pathological alterations of the lipid balance in cellular membranes. Several groups have reported intense lipid peroxidation in the skin and blood of vitiligo patients, based on the increased levels of MDA and diene conjugates (13, 46).

[1]Tissue Engineering and Cutaneous Pathophysiology Laboratory and [6]2nd Dermatology Department, Dermatology Research Institute (IDI IRCCS), Rome, Italy.
[2]Biochemistry Department, Byelorussian State University, Minsk, Byelorussia.
[3]Department of Biomedical Sciences, University of Siena, Siena, Italy.
[4]Department of Food and Nutrition, Keyung Hee University, Seoul, Korea.
[5]Biophysics Department, Institute for Physical Chemical Medicine, Moscow, Russia.

According to the current view, the dramatic decrease of the activity of epidermal catalase (CAT), reproducibly observed in the vitiligo depigmented lesions (12, 35, 36), further aggravates the condition, and allows the maintenance of extremely high, millimolar epidermal concentrations of H_2O_2 (35). The same authors have explained impaired CAT activity in terms of H_2O_2-dependent inactivation of the enzyme, occurring in the presence of such toxic levels of its own substrate. The recent findings of single nucleotide polymorphisms (SNPs) in the *CAT* gene of vitiligo patients (7) led to a further suggestion, that genetically modified catalase may be more susceptible to oxidative inactivation by H_2O_2 (44). However, possible nontoxic effects of disturbed redox control, derived from the H_2O_2–CAT imbalance on skin cell functions, have never been taken into account. In particular, no author considered the two redox-dependent interconnected regulatory factors, glutathione S-transferases and 4-hydroxy-2-nonenal (HNE), important for cellular adaptation to a variety of genotoxic, metabolic, and oxidative stresses (4, 18, 41), as pathogenically implicated in vitiligo. HNE is a stable product of lipid peroxidation, easily reacting with proteins and DNA, thus possessing important regulatory properties towards cell growth and differentiation (31), as well as towards cellular death and survival (19, 41). HNE homeostasis in the organism is controlled by GSTs, a family of conjugating enzymes playing a key role in the phase II biotransformation of organic xenobiotics, in the metabolism of endogenous electrophils, including HNE, and in the deactivation of ROS, that are involved in cellular processes of inflammation and degenerative diseases (4, 18, 45). Of note, HNE can be a substrate for GST, either inhibiting enzyme activity, or regulating its expression, depending on concentration (18). As regards CAT, HNE may target the enzyme, inducing its deactivation (14) and neoantigen formation (23). GSTs, and in particular the isoform GSTM1, exert several nonenzymatic functions relevant to programmed cell death (10), to the control of intracellular NO levels, acting as a NO carrier (8), to the direct regulation of kinase pathways (40), to iNOS upregulation through NFkB translocation (45), and other cellular functions.

An independent line of research related to the vitiligo "puzzle" focuses the key role of keratinocytes in the survival and functions of melanocytes. Keratinocyte-produced cytokines may promote or inhibit melanocyte life span, proliferation, and melanogenesis (20). Vitiligo keratinocytes, tightly connected with melanocytes in a keratinocyte–melanocyte unit, display a characteristic impairment of structure and functions (5, 24). Lower-than-normal levels of melanocyte-stimulating growth factors, such as basic fibroblast growth factor (bFGF) and stem cell factor (SCF) (24, 26), and significantly higher levels of the potential inhibitors of melanocyte growth TNF-α, IL-1α, and IL-6, have been detected in the depigmented areas of vitiligo skin (20, 26). There is steadily growing evidence that the production of cytokines, their interaction with receptors, and cell responses to cytokines are under redox control (3, 15, 33, 37).

Here, we describe nontoxic regulatory functions of local and generalized redox imbalance in the blood components of vitiligo patients and in the cultivated keratinocytes derived from depigmented and normally pigmented areas of vitiligo skin. We demonstrated for the first time dramatic alterations of both HNE-protein adduct levels and GSTM1 and GSTT1 expression in vitiligo. Hence, we focused primarily on the HNE-GST couple and its effects on H_2O_2 metabolism and cytokine production. Vitiligo conditions were partially reproduced *in vitro* by adding exogenous HNE to cultures of normal human keratinocytes.

Materials and Methods

Patients and controls

Forty-nine vitiligo patients with general characteristics collected in Table 1 were recruited in the study, and twenty-six healthy subjects of matching age and sex were included as controls. The local Ethics Committee of the Dermatology Research Institute (IDI IRCCS, Rome, Italy) approved the clinical-laboratory study, carried out in a strict compliance with Helsinki Declaration on human experiments. Venous blood and skin biopsies were taken with patient's informed consent.

Cell cultures and treatments

Full-thickness skin biopsies were taken from pigmented and depigmented body areas of vitiligo patients (n = 3), and from healthy age- and sex-matched donors (n = 3). Epidermal cells were cultured on a feeder-layer of lethally irradiated 3T3-J2 mouse fibroblasts (16). Briefly, biopsies were minced and trypsinized (0.05% trypsin/0.01% ethylene diamine tetraacetate, sodium salt) at 37°C for 3 h. Cells were collected every 30 min, plated ($4\times10^4/cm^2$) on lethally irradiated 3T3-J2 fibroblasts ($2.4\times10^4/cm^2$), and cultured in humidified atmosphere containing 5% CO_2. Culture medium was a 2:1 mixture of Dulbecco's modified Eagle's medium (DMEM) and Ham's F12 medium, containing fetal calf serum (FCS, 10%), insulin (5 μg/ml), adenine (0.18 m*M*), hydrocortisone (0.4 μg/ml), cholera toxin (0.1 N*M*), triiodothyronine (2 N*M*), epidermal growth factor (EGF, 10 ng/ml), penicillin-streptomycin (50 Iu

Table 1. General Characteristics of the Groups of Patients and Control Subjects

Group	*Number*	*Gender, F/M*	*Age, years (range)*	*Concomitant autoimmune diseases (number of patients)*	*Stable/Active form*	*Duration, years (range)*
Vitiligo	49	30 F 19 M	37.5 ± 18.2 (10–66 y)	Thyroiditis, 14 Alopecia areata, 4 Ulcer colitis, 1 Psoriasis, 2	4/45	14.2 ± 10.5 (0.5–40 y)
Controls	26	18 F 8 M	36.2 ± 8.1 (28–50 y)	–	–	–

to 50 μg/ml), and glutamine (4 m*M*). One day after confluence, primary cultures were trypsinized, plated in secondary cultures at a density of $4\times10^4/cm^2$ in the presence of lethally irradiated 3T3-J2 cells ($2.4\times10^4/cm^2$), and further cultivated as above. Keratinocytes in their fourth *in vitro* passage were used for the experiments.

A pure melanocyte population was isolated from human foreskin specimens obtained during circumcision surgery (n = 1). Epidermal cultures were performed as described above. Three days after confluence, cultures in secondary passage were trypsinized, and the cell suspension ($4\times10^4/cm^2$) was cultivated without feeder-layer in melanocyte growth medium, a 2:1 mixture of DMEM and Ham's F12 media, containing FCS (5%), insulin (5 μg/ml), adenine (0.18 m*M*), hydrocortisone (0.4 μg/ml), cholera toxin (0.1 N*M*), triiodothyronine (2 N*M*), epidermal growth factor (10 ng/ml), penicillin-streptomycin (50 Iu to 50 μg/ml), glutamine (4 m*M*), bFGF (1 ng/ml), and phorbol 12-myristate 13-acetate (PMA, 10 ng/ml). Twenty-four hours after seeding, medium was changed, free-floating cells were removed, and geneticin (100 μg/ml) was added for 2–4 days in the case of fibroblast growth. After 2–3 passages in culture, melanocytes were isolated, characterized for a 100% positivity to 3,4 dihydroxyphenylalanine (L-DOPA) staining, and used for the co-culture experiments.

To prepare co-cultures, keratinocytes reaching confluence were seeded with heterologous melanocytes, which were added in a physiological 1/40 melanocyte/keratinocyte ratio (5), and cultivated in complete keratinocyte medium without bFGF and PMA, in the presence of lethally irradiated 3T3-J2 cells ($2.4\times10^4/cm^2$). The co-cultures plated in parallel 24- and 6-multiwell plates were characterized by the phase-contrast microscopy, L-DOPA staining and Western blot. The process of co-culture preparation is shown in Figure 1A.

For UV and HNE exposure experiments, serum-starved for 24 hours keratinocytes were subjected to standardized UVA+UVB irradiation (Solar Simulator, Dermalight Vario with filter A2, Dr. Hoehnle AG, UV Technology, Planegg, Germany). Application of the A2 filter produced a UVA (90%) and UVB (10%) irradiation. The emission spectrum started from 300 nm, with the emission peak at 375 nm. The light effluence rate on the cell monolayer was 33 mW/cm^2, the length of the exposure was 30 s, the dose 1.1 j/cm^2. At 1 h after irradiation (recovery period), conditioned medium was collected and cells were detached by addition of trypsin/EDTA, washed in PBS, quickly frozen, and stored at -80°C until gene expression analysis.

In the experiments with HNE (Cayman Chem. Co., Ann Arbor, MI), a 25 μ*M* HNE solution in dimethyl sulfoxide, or dimethyl sulfoxide alone (control) were added to each well. After 1 and 4 h of incubation, the conditioned medium was collected for further cytokine assay. Keratinocytes were processed for RNA isolation and analysis. All exposure experiments were replicated three times, and measurements were done in triplicate. Results were expressed in percent of the corresponding control values, as mean $\pm$ S.D.

Blood sampling and processing

Peripheral venous blood (10 ml) was drawn into vacutainers with ethylene-diamino-tetra-acetic acid disodium salt as anticoagulant. Aliquots of whole blood were used immediately to monitor luminol-dependent chemiluminescence (LDCL) as a measure of ROS. The remaining blood was centrifuged at 3000 rpm for 10 min to separate plasma and erythrocytes, both subsequently aliquoted and stored at -80° C until assayed.

Redox parameters in peripheral blood components, cultured keratinocytes, and keratinocyte–melanocyte co-cultures

Fresh blood (10 μl) was diluted in 1 ml of pre-heated Hanks' Balanced Salt Solution (pH 7.4) containing 0.2 m*M* luminol. After PMA (10 ng/ml) addition, and the LDCL response was monitored for 5 min (6) with a Victor^2 (Wallac Oy) 1420 multilabel counter, equipped with Wallac 1420 Software, Perkin Elmer. Each measurement was repeated three-five times. Results were expressed in counts per second (cps) per μl of blood. Hydrogen peroxide in the conditioned medium was determined by the Hydroperoxide Assay kit (Sigma, Milan, Italy). The results were expressed as nmoles of H_2O_2/mg protein. Intracellular H_2O_2 production was determined by 2′,7′-dichlorofluorescein diacetate staining (41) followed by microscopy photo-imaging. The levels of NO_2^-/NO_3^- in the blood plasma and in the conditioned medium were determined by the Griess reagent, following manufacturer's instructions (Cayman Chemical Co. Ann Arbor, MI). Quantitative analysis of reduced glutathione (GSH) and its oxidized form (GSSG) in erythrocytes and keratinocytes was carried out by high pressure liquid chromatography (32) on a Shimadzu chromatograph equipped with a photodiode array detector, and a analytical Supelcosil LC-NH_2 column (25 cm $\times$ 4.6 mm, 5 μm), with the analytical parameters here described. Detection: 355 nm; mobile phase A = MeOH/H_2O (65/35, v/v), B = X/Y (20/80, v/v), where X is sodium acetate $3H_2O$, 272 g - CH_3COOH, 372 ml - H_2O, 122 ml, and Y is MeOH/H_2O 80/20 (v/v). Gradient program: %B 5 for 15 min, %B 90 in 30 min, and then %B 90 for 45 min; flow 1 ml/min. Results were expressed as mg/l of erythrocytes or as mg/mg of keratinocyte protein.

For enzymatic analyses, lysates of erythrocytes or cultured human skin cells were prepared. Erythrocytes were lysed in hypotonic solution, keratinocytes or the keratinocyte–melanocyte mixtures were subjected to five freeze-thaw cycles, and the post-spin cell lysates were analyzed. Erythrocyte and keratinocyte Cu,Zn-SOD activity was measured spectrophotometrically at 505 nm using Cayman Chemical kits. Total GST activity was measured spectrophotometrically by the methods described previously, using chloro-2,3-dinitrobenzene (17) or HNE (2) as substrates. CAT activity was detected by the Aebi method (1). Erythrocyte GPx was determined using Cayman Chemical kits, according to the method (28). Protein content was measured according to Bradford, using Bio-Rad (Hercules, CA) microplate assay kit.

HNE–protein adducts in peripheral blood plasma and cultured keratinocytes

For Western blot analysis, plasma samples or keratinocyte lysates (60 μg protein, determined by Bio-Rad protein assay) were diluted in reducing sample buffer and boiled for 10 min. Samples were resolved on a 4%–20% sodium dodecyl sulphate (SDS)-polyacrylamide gradient gel (Invitrogen, Milan, Italy), and electro-transferred onto nitrocellulose membranes. After blocking in 3% fat-free milk in phosphate-buffered saline

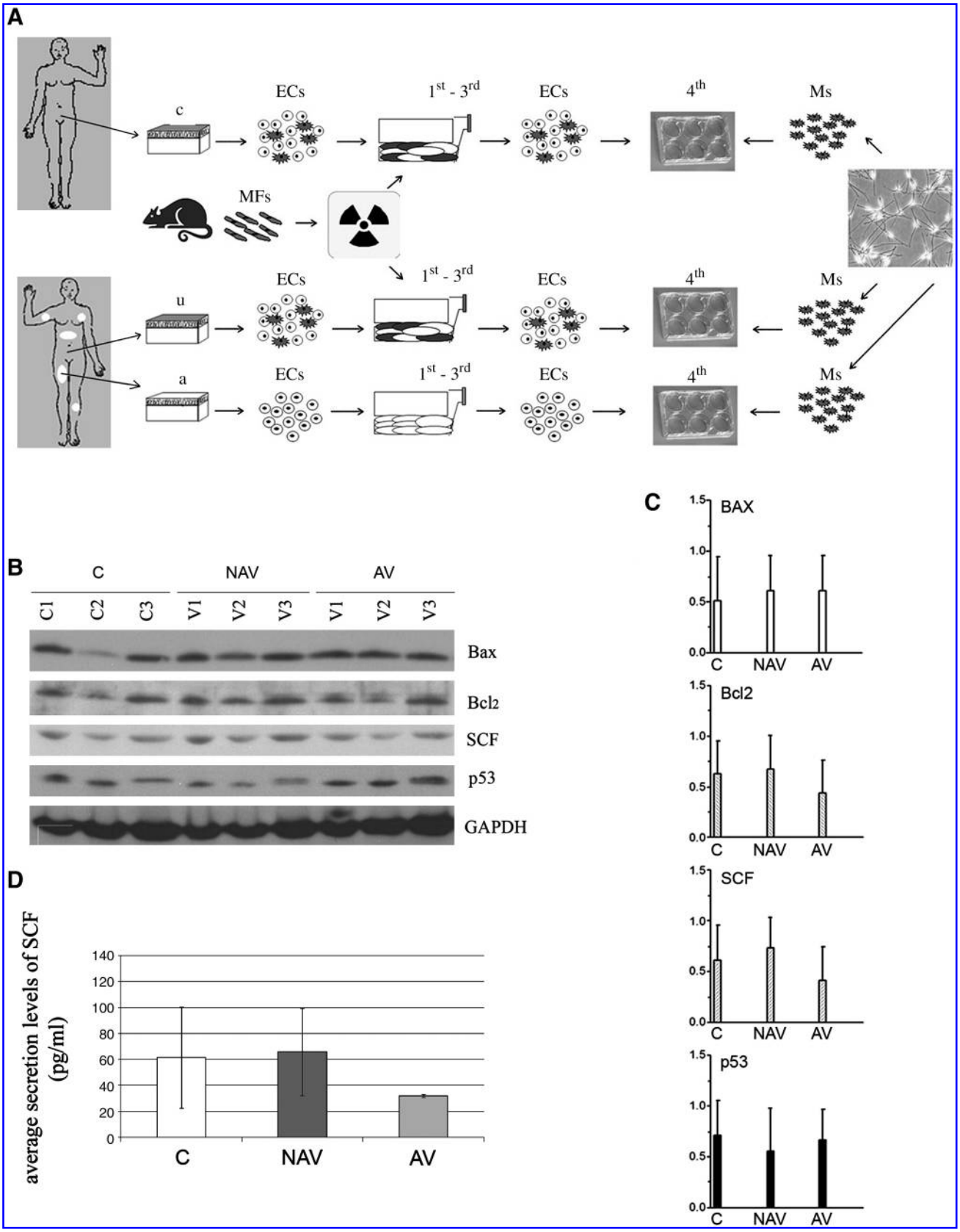

FIG. 1. Experimental design and characteristics of keratinocyte–melanocyte co-cultures. (**A**) Epidermal cells (ECs) derived from skin biopsies obtained from healthy donors and affected (depigmented) and nonaffected (pigmented) areas of vitiligo patients were cultivated on the lethally irradiated murine fibroblasts (MFs) for three passages. Normal allogeneic melanocytes (Ms) were then added to keratinocyte cultures; keratinocyte–melanocyte co-cultures were cultivated for one more passage (4^{th} passage), and then analyzed. (**B**, **C**) Western blots and corresponding densitometry bars for Bax, Bcl_2, SCF, and p53 proteins. (**D**) ELISA analysis of SCF in the conditioned medium. AV, affected vitiligo keratinocytes/co-cultures; C, control keratinocytes/co-cultures; NAV, nonaffected vitiligo keratinocytes/co-cultures.

solution, the membranes were incubated overnight at 4°C with goat anti-HNE polyclonal antibodies (Millipore, Billerica, MA) at 1:3000 dilution. After washing, mouse anti-goat horseradish peroxidase-conjugated antibodies (Santa Cruz Biotechnology, Inc., Santa Cruz, CA) were used as secondary antibodies. Membranes were processed with the enzymatic chemiluminescence solution (ECL, Immune-Star™ HRP Substrate Kit, Bio-Rad), and exposed to photographic film (Hyperfilm™ECL™, Life Science, Amersham Biosciences, Milan, Italy), according to manufacturer recommendations. Band densities were quantified using the National Institute for Health image shareware. Results of three independent experiments were expressed in arbitrary units, as mean values ± SD.

Assay for cytokine levels in peripheral blood plasma, cultured keratinocytes, and keratinocyte–melanocyte co-cultures

Cytokine levels in blood plasma and conditioned medium of skin cells cultures were determined by multiplexed analysis using the Bio-Plex Suspension Array System (Bio-Rad Laboratories) panel detecting simultaneously the levels of 27 cytokines, chemokines, and growth factors: IL-1β, interleukin 1 receptor antagonist (IL-1ra), IL-2, IL-4, IL-5, IL-6, IL-7, IL-8, IL-9, IL-10, IL-12, IL-13, IL-15, IL-17, eotaxin, basic fibroblast growth factor (bFGF), granulocyte colony stimulating factor (G-CSF), granulocyte macrophage colony stimulating factor (GM-CSF), interferon gamma (IFNγ), interferon gamma-produced protein of 10 kDa (IP-10), monocyte chemotactic protein 1 (MCP-1), macrophage inflammatory proteins (MIP-1α and MIP-1β), regulated upon activation, normal T-cell expressed, and secreted (RANTES), the platelet-derived growth factor disulfide-bonded B chain homodimer (PDGFbb), tumor necrosis factor alpha (TNFα), and vascular endothelial growth factor (VEGF). The assay was performed according to the manufacturer's instructions. Cytokine concentrations were expressed in pg/ml of plasma, or pg/mg of protein in the aqueous scale extract, and each factor was quantified in the linear range of its calibration curve using a Bio-Rad array reader. Cytokine concentrations were determined on a Bio-Rad array reader using the linear parts of corresponding calibration curves, and were expressed in pg/mL plasma or pg/mg of keratinocyte protein.

Quantitative real-time-PCR in cultured keratinocytes

Total RNA was isolated from frozen keratinocytes using the GenElute^{TM} Mammalian Total RNA Kit from Sigma (Milan, Italy), following the manufacturer's instructions. The amount of RNA was determined by absorbance at 260 nm. Total RNA (1 μg) was reverse-transcribed using the iScript cDNA Synthesis Kit (Bio-Rad), at 25°C for 5 min, then at 42°C for 30 min, and finally at 85°C for 5 min, in a final reaction volume of 40 μl. Amplification of cDNA was performed with iQTM Supermix, using the MiniOpticon Real-Time PCR Detection System (Bio-Rad). All real time assays were carried out under the following conditions: 35 cycles of denaturation at 95°C for 15 sec, annealing and extension at 60°C for 60 sec. Melt curve analysis was performed to confirm the specificity of the amplified products. All samples were run in triplicate, and relative expression was determined by normalizing samples to β-actin and 18S rRNA as housekeeping genes.

The following primer sets were designed using Primer-BLAST (NCBI) and synthesized by Eurofins MWG Operon (Ebersberg, Germany): β-actin fwd: 5′-AATCTGGCACCA CACCTTCTAC-3′; β-actin rev: 5′-ATAGCACAGCCTGGA TAGCAAC-3′; 18S rRNA fwd: 5′- TCCCCCAACTTCTTA GAGG-3′; 18S rRNA rev: 5′- GCTTATGACCCGCACTTAC-3′; iNOS fwd: 5′- TACTCCACCAACAATGGCAA-3′; iNOS rev: 5′- ATAGCGGATGAGCTGAGCAT-3′; IL-6 fwd: 5′-GT GTGAAAGCAGCAAAGAG-3′; IL-6 rev: 5′-CTCCAAAAGA CCAGTGATG-3′; TNF-α fwd: 5′- TCCTTCAGACACCCTC AACC-3′; TNF-α rev: IL-1α fwd: 5′-TGGCTCATTTTCCCTC AAAAGTTG-3′; IL-1α rev: 5′-AGAAATCGTGAAATCCGAA GTCAAG-3′; GSTT1 fwd: 5′- CGCTGTTTACATCTTTGCCA-3′; GSTT1 rev: 5′- ACCTTCTTGAGGGGGTTCAC-3′; GSTM1 frw: 5′- TTCCCAATCTGCCCTACTTG -3′; GSTM1 rev: 5′-TCTCCTCTTCTGTCTCCCCA-3′; GSTP1 frw: 5′- ACCTCCG CTGCAAATACATC -3′; GSTP1 rev: 5′- GGGCAGTGCCTT CACATAGT-3′; bFGF frw: 5′- TCAAAGGAGTGTGTGCTA AC-3′; bFGF rev: 5′- ATACTGCCCAGTTCGTTTC-3′; COX-2 frw: 5′-TTCTCCTTGAAAGGACTTATGGGTAA-3′; COX-2 rev: 5′-AGAACTTGCATTGATGGTGACTGTTT-3′; PDGFbb frw: 5′- TGCTGTTGAGGTGGCTGTAG -3′; PDGFbb rev: 5′-AATCAGAGTGGAGTGTGGGG-3′; CAT frw: 5′- CGTCCTG AGTCTCTGCATCA -3′; CAT rev: 5′- TTTGCAATAAACT GCCTCCC -3′.

Western blot analysis

For immunoblots, confluent keratinocyte + melanocyte co-cultures were lysed for 30 min on ice in radioimmune-precipitation assay buffer, equal amounts of samples were electrophoresed on 12.5% SDS–polyacrylamide gel. Western blots were performed with the following antibodies: anti-p53 and anti-SCF from Santa Cruz Biotechnology, Inc.; anti-Bax(Polyclonal) and anti-Bcl2(Polyclonal) from BD Biosciences (San Jose, CA). To determine expression of GST isoforms, protein extracts (2 μg for GST P1-1 and 20 μg for GST M1-1 and A1-1 detection) were separated on reducing SDS 12% polyacrylamide gel electrophoresis, and then transferred overnight onto a Hybond polyvinylidene difluoride nylon membrane at 20 V constant with an Invitrogen (Carlsbad, CA) transblot apparatus. The membranes were incubated with polyclonal primary anti- GST P1-1, GST M1-1, GST A1-1 antibodies (Calbiochem, Darmschtadt, Germany), diluted 1:2000 in PBS buffer containing 0.5% Tween 20 and 0.1% skimmed milk for 2 h. After a wash step, they were finally incubated for 40 min with horseradish peroxidase conjugated with anti-rabbit IgG diluted 1:5000 in PBS buffer, to detect the immunoreactions. Protein expression was normalized by glyceraldehyde 3-phosphodehydrogenase expression level, and shown as photographs of protein bands, with optical density values of each band. The final data were expressed as percent of normal values.

Measurement of protein phosphorylation

Spontaneous and UV-induced phosphorylation of protein kinase B (Akt1) and p53 was quantified by modified cell-based ELISA assays without protein isolation using CASE™ Kit (SABiosciences Co., Frederick, MD). Before analysis, keratinocytes were fixed with 4% formaldehyde. The degree of ERK1/2 and Akt phosphorylation in keratinocytes exposed to HNE was examined by Western blot analysis using

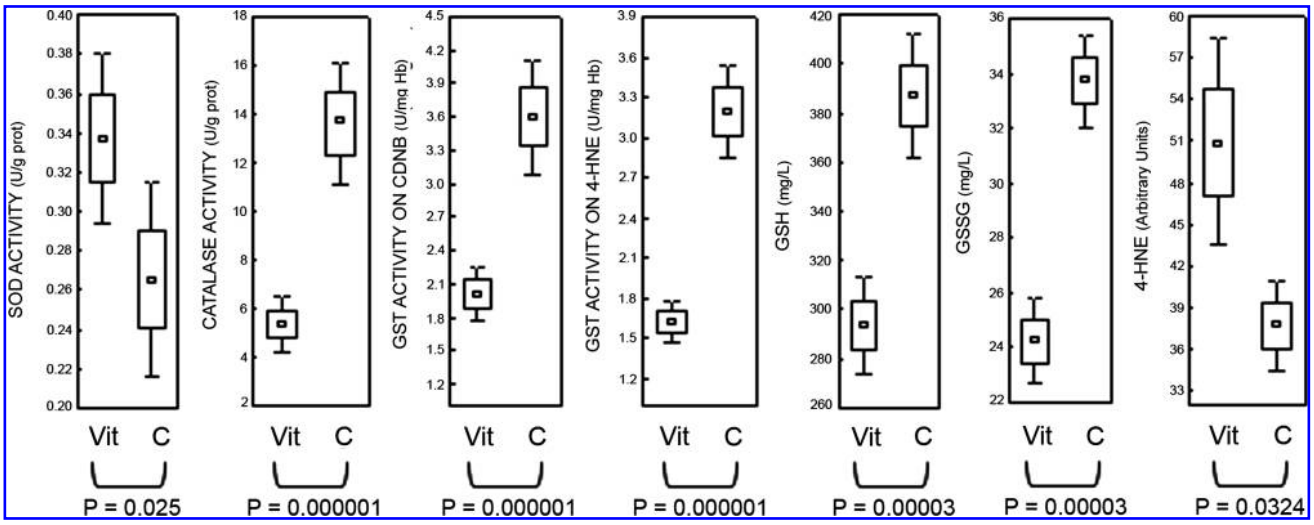

FIG. 2. Redox parameters in the blood components of vitiligo (Vit) patients and healthy donors (C). The activities of CuZnSOD, catalase, GST (CDNB and HNE), and GSH/GSSG levels were measured in erythrocytes. HNE–protein adducts were determined in the blood plasma. Values are presented as mean (□), standard error of the mean (*upper and lower limits of the box*), 1.96×standard error (*upper and lower wiskers*). Intergroup significant differences ($p < 0.05$ or 0.01) are reported under each panel.

anti-phosphoERK1/2 and anti-phospho-Akt antibodies from Cell Signaling Technology (Beverly, MA), and the bands obtained were quantified and normalized to the corresponding total nonphosphorylated signals by densitometry.

Statistics

Statistical analysis of clinical laboratory data was performed using STATISTICA 6.0 program from StatSoft Inc. (Tulsa OK). Reported values were treated as continuous. Normality of data was checked using the Shapiro–Wilk test. Since data distribution was significantly different from normal, nonparametric statistics was used. Values of redox parameters in the blood components were presented as mean, standard error of the mean, 95% confidence interval (1.96×standard error). Mann–Whitney U-test for independent samples was employed for comparison between patients and controls.

All biochemical and molecular measurements in skin cell cultures were done in triplicate, and data of at least three independent experiments were statistically evaluated. To assess the difference between experimental groups, two-tailed Student's *t*-test was applied and *P* values <0.05 were considered to be significant. Statistical evaluation of HNE-protein adduct data was performed using one-way analysis of variance. Differences were considered significant if $P < 0.01$.

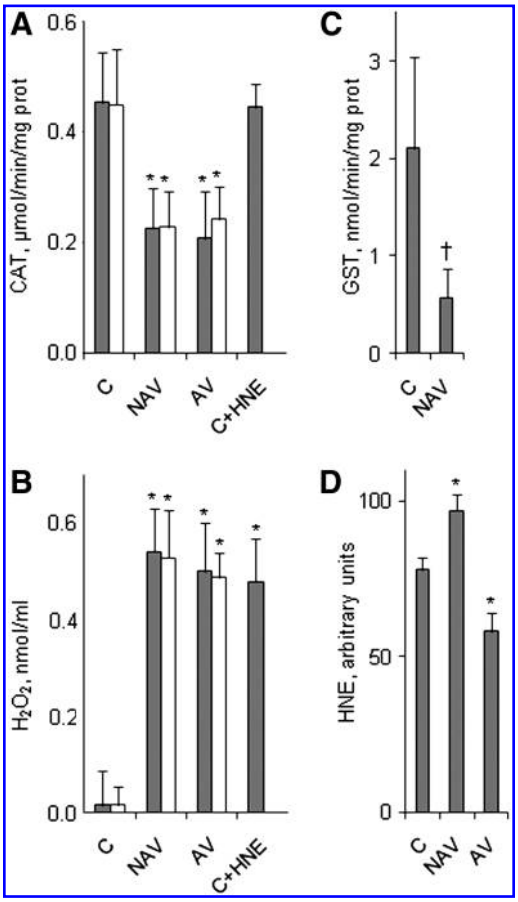

FIG. 3. Redox parameters in cultivated keratinocytes and their co-cultures with allogeneic melanocytes. (**A**) Catalase activity in keratinocytes (*black bars*) and keratinocyte/melanocyte co-cultures (*empty bars*). (**B**) Hydrogen peroxide levels in the conditioned medium. (**C**) Glutathione S-transferase activity towards HNE. (**D**) HNE-protein adducts in keratinocytes. Western blot analysis of keratinocyte lysates showed three bands at 48, 85, and 117 kiloDalton. The three bands for each experimental group were quantified by densitometry and summarized. AV, keratinocytes derived from affected vitiligo skin; C, keratinocytes of donors; C+HNE, control keratinocytes treated with 25 μM HNE for 4 h; NAV, keratinocytes derived from nonaffected vitiligo skin; $^{\dagger}p < 0.01$ and $^{*}p < 0.05$ vs. control cultures.

Results

Peripheral blood of vitiligo patients displays distinct biochemical markers of redox imbalance: Low CAT and GST activities, low GSH and GSSG levels in erythrocytes, and high plasma levels of HNE-protein adducts

Out of ten parameters of redox balance determined in the blood plasma and erythrocytes (whole blood chemiluminescence, plasma levels of NO_2^-/NO_3^- and HNE-protein adducts, reduced glutathione (GSH) and oxidized glutathione (GSSG) levels in erythrocytes, and CAT, GST (towards 1-chloro-2,4-dinitrobenzene (CDNB), and HNE substrates), CuZnSOD, and GPx activities in erythrocytes), seven were statistically significantly different in vitiligo patients when compared to the control group (Fig. 2). As expected, CAT activity was lower in erythrocytes of vitiligo patients as compared to age-matched controls. Erythrocyte GST activity measured with either CDNB or HNE as substrates was remarkably lower than normal, and plasma levels of HNE–protein adducts in vitiligo were statistically higher than the control values. Both GSH and GSSG levels were lower, and CuZnSOD activity was higher than normal in the vitiligo erythrocytes. At the same time, whole blood PMA-activated LDCL (363 ± 22 cps/μl and 425 ± 57 cps/μl, $P = 0.612$), plasma nitrites/nitrates levels ($22.7 \pm 2.2\,\mu M$ and $19.0 \pm 3.3\,\mu M$, $P = 0.138$), and erythrocyte GPx activity (27.3 ± 1.2 U/mg Hb and 25.0 ± 1.6 U/mg Hb, $P = 0.224$) were not statistically different for the vitiligo and control groups, respectively.

Redox imbalance features in the cultures of affected and nonaffected vitiligo keratinocytes and in their co-cultures with normal melanocytes

Preliminary analysis of keratinocyte–melanocyte co-cultures showed that at the fourth passage cultures of normal (C), affected (AV), or nonaffected (NAV) vitiligo keratinocytes contained similar numbers of allogeneic melanocytes, as revealed by DOPA-staining (67.5 ± 12.7, 51.8 ± 19.2, and 56.7 ± 13.7, for C, NAV, and AV, respectively). Western blot analysis of pro-apoptotic p53, anti-apoptotic Bcl_2 and Bax proteins, and SCF did not reveal statistical difference between the cultures studied (Figs. 1B and 1C). ELISA assay of SCF in the conditioned medium also did not show statistically significant difference (Fig. 1D).

At the same time, several biochemical parameters of redox status were dramatically different in the vitiligo and control cultures/co-cultures. CAT activity and GST activity towards

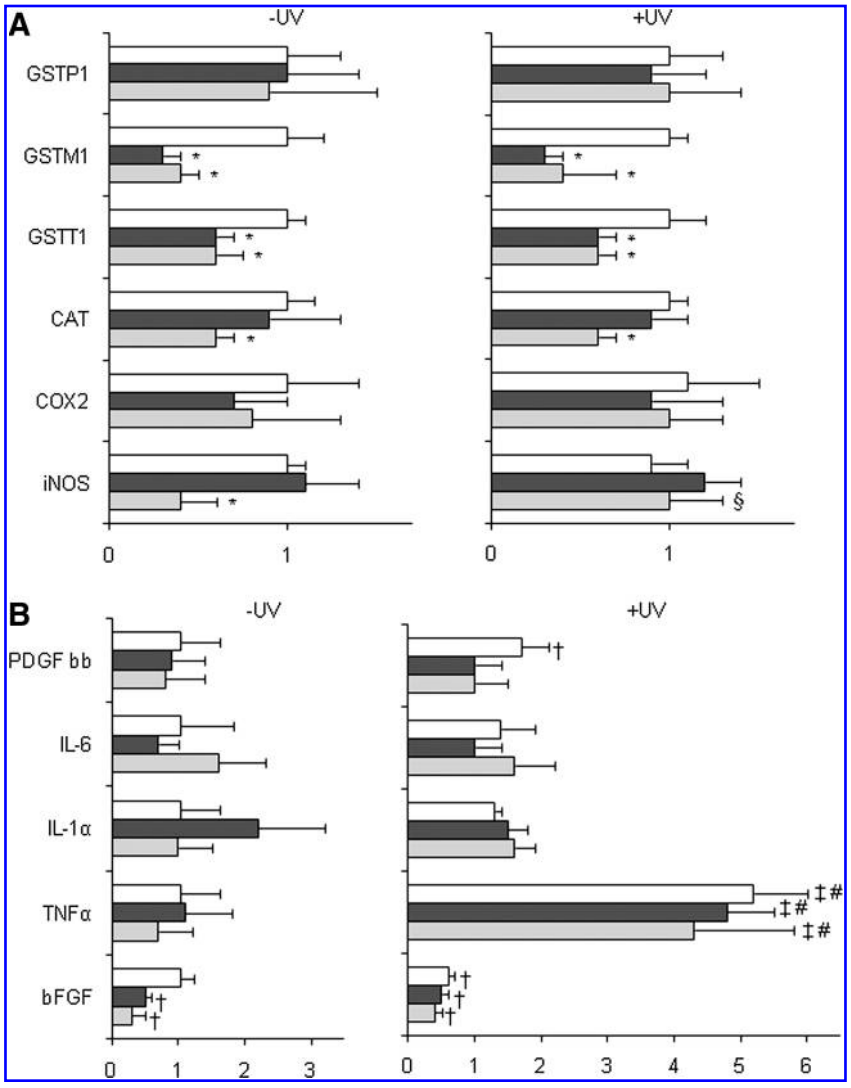

FIG. 4. Gene expression in cultivated control (*empty bars*), nonaffected (*black bars*), and affected (*gray bars*) vitiligo keratinocytes. (**A**) Relative spontaneous (-UV) and UV-induced (+UV) expression of redox enzyme genes versus control nonirradiated keratinocytes. Cells were processed for qRT-PCR analysis 1 h after exposure to UVA+UVB irradiation. $^{*}p < 0.05$ *vs.* control keratinocytes; $^{\S}p < 0.01$ *vs.* corresponding non-irradiated keratinocytes. (**B**) Relative spontaneous (-UV) and UV-induced (+UV) expression of cytokine genes versus control nonirradiated keratinocytes. $^{\dagger}p < 0.05$ and $^{\ddagger}p < 0.01$ *vs.* control nonirradiated keratinocytes; $^{\#}p < 0.01$ *vs.* corresponding nonirradiated keratinocytes.

HNE were significantly lower, and intracellular (data not shown) as well as extracellular H_2O_2 levels remarkably higher-than-normal in vitiligo keratinocytes, independently of the skin area where the cells derived from, and of mono- or co-culture conditions (Fig. 3). However, even if highly increased in vitiligo cells, H_2O_2 levels remained within a nontoxic micromolar range of concentrations. On the other hand, HNE–protein adduct levels were higher in NAV than in AV or control keratinocytes (Fig. 3). Other redox parameters, such as CuZnSOD, GST activity on CDNB, GSH, and NO_2^-/NO_3^- levels, were similar for all cultures/co-cultures studied (data not shown). Spontaneous gene expression of iNOS, CAT, and both GSTM1 and GSTT1 isozymes was remarkably repressed in AV keratinocytes as compared to control cells. In NAV keratinocytes, exclusively GSTM1 and GSTT1 genes were statistically significantly down-regulated (Fig. 4A).At the same time, baseline expression of GSTP1, GSTA1, and SOD2 genes was similar in all cultures studied (data not shown). Western blot analysis of different GST isoforms demonstrated the highly suppressed GSTM1 protein expression in both AV and NAV keratinocytes cultivated either alone or in the presence of normal melanocytes (Fig. 5A). No differences resulted for GSTA1 and GSTP1 proteins, between normal and vitiligo keratinocytes or keratinocyte/melanocyte co-cultures. Similarly, Western blot analysis did not reveal any abnormalities in the expression of CAT protein in both AV and NAV keratinocytes (data not shown).

Blood plasma and both affected and nonaffected cultured keratinocytes of vitiligo patients display abnormal cytokine pattern

Levels of 9 out of 27 cytokines were drastically dysregulated in the cultures of keratinocytes derived from AV or NAV skin areas (Figs. 6A–6C). Thus, levels of IL-8, bFGF, and MCP-1 were significantly lower than normal in AV keratinocytes. Conversely, the levels of IL-6, IL-7, IL-8, G-CSF, PDGFbb, IP-10, and VEGF were highly increased in NAV cells. AV keratinocytes displayed intermediate levels of PDGFbb and VEGF and remarkably increased levels of G-CSF and IP-10 as compared to NAV cells. Similar results were obtained in keratinocyte–melanocyte co-cultures (data not shown). The plasma levels of IL-8, MCP-1, and TNF-α were significantly lower in the vitiligo *vs.* the control group (Fig. 6D). The other plasma cytokines were not dysregulated.

With regard to spontaneous cytokine gene expression, only bFGF gene was downregulated in both NAV and AV keratinocytes (Fig. 4B), while expression of TNF-α, IL-6, IL-1ß, and PDGFbb genes was similar in all three types of keratinocytes.

Exposure of vitiligo keratinocytes to mild UVA+UVB irradiation results in the induction of impaired spontaneous iNOS but not CAT, GSTM1, and GSTT1 gene expression, and abolishes the differences in bFGF gene expression between control and vitiligo keratinocytes

Exposure of cultured keratinocytes to mild nontoxic UV light simulating solar irradiation resulted, after 1 h of recovery, in multiple molecular consequences, such as the induction of spontaneous iNOS gene expression, inhibited in AV keratinocytes, whilst it did not affect the spontaneously suppressed *CAT*, *GSTM1* and *GSTT1* genes in all vitiligo cultures (Fig. 4A). Concerning cytokine gene expression, UV irradiation remarkably and similarly induced *TNF-α* in all cell types studied (Fig. 4B). Since UV irradiation inhibited spontaneous *bFGF* gene expression in normal keratinocytes, and slightly induced it in AV cells, the expression of the gene became statistically indistinguishable in normal, NAV, and AV cells.

Spontaneous and UV-induced p53 phosphorylation is higher and UV-induced Akt1 phosphorylation is lower in vitiligo versus normal keratinocytes

Spontaneous and UV-induced activation of intracellular pathways regulating cell survival and response to external alarms was different for normal and vitiligo keratinocytes.

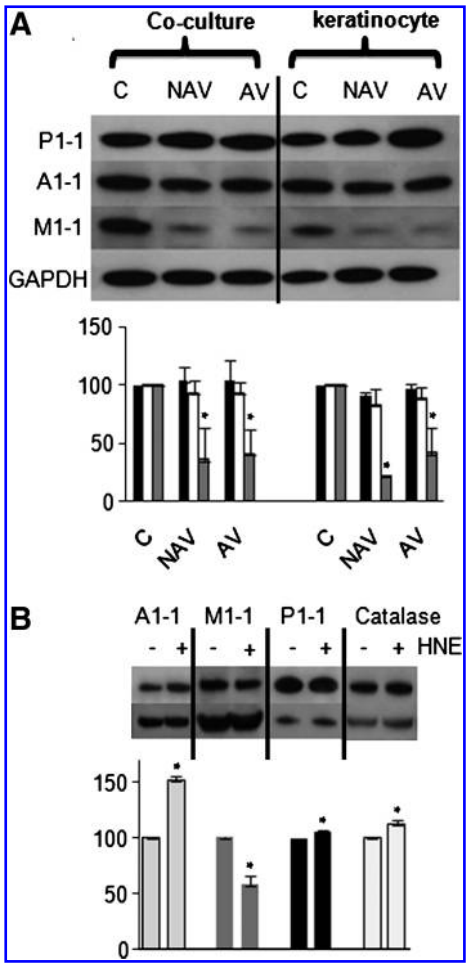

FIG. 5. Protein expression of GST isozymes in keratinocytes and their co-cultures with allogeneic melanocytes. (**A**) Western blots and densitometry of GSTA1-1, GSTP1-1, and GSTM1-1 proteins normalized by the glyceraldehyde 3 phosphate dehydrogenase (GAPDH) protein levels in the same line. AV, affected vitiligo keratinocytes/co-cultures; C, control keratinocytes/co-cultures; NAV, nonaffected vitiligo keratinocytes/co-cultures; $^*p < 0.009$. (**B**) Western blots and densitometry of GST isozymes (GSTA1-1, GSTP1-1, and GSTM1-1) and catalase in the control keratinocytes incubated with (+) HNE (25 μM) or without (-) HNE for 4 h. The *upper line* of spots represents proteins normalized by GAPDH. $^*p < 0.002$.

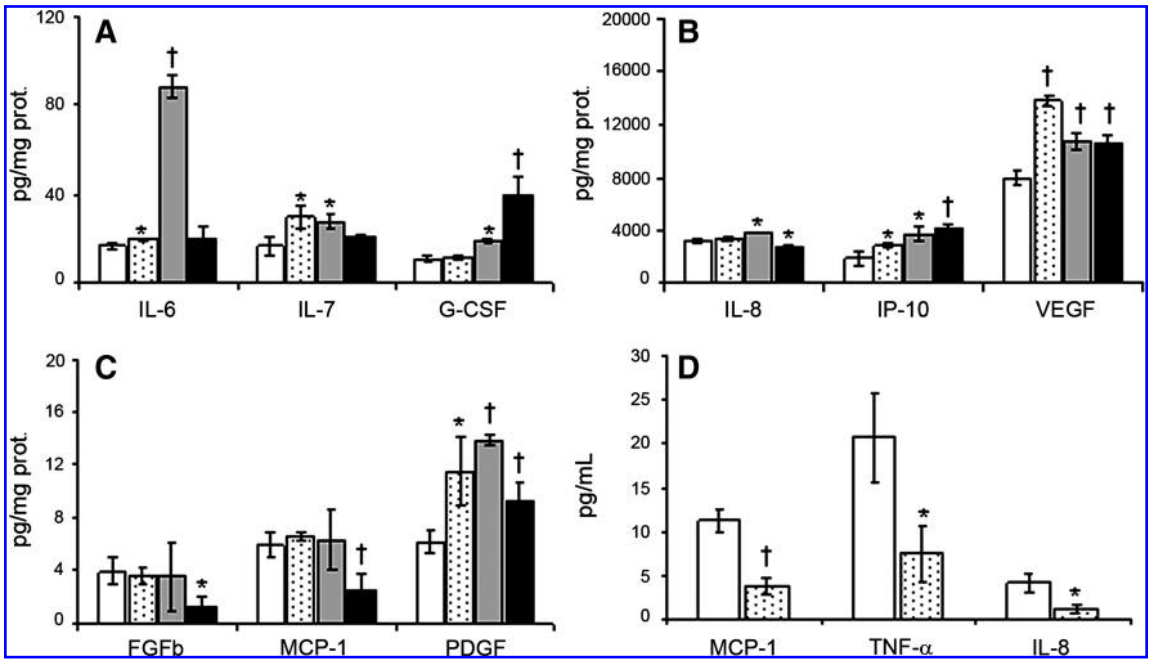

FIG. 6. Cytokine levels in the conditioned medium of keratinocyte cultures and blood plasma. (**A–C**) Concentration of cytokines (pg/mg protein) in the conditioned medium of control keratinocytes (n = 3, *empty bars*), control keratinocytes incubated with HNE (25 μM) for 4 h (n = 3, *dotted bars*), nonaffected vitiligo keratinocytes (n = 3, *gray bars*), and affected vitiligo keratinocytes (n = 3, *black bars*). Each measurement was repeated three times and data are expressed as mean ± SD. $^{*}p < 0.05$ and $^{\dagger}p < 0.01$ *vs.* control keratinocytes. (**D**) Plasma concentration of cytokines (pg/ml) in healthy donors (n = 26, *empty bars*) and vitiligo patients (n = 46, *dotted bars*). Plasma samples were run in duplicates and data are expressed as mean ± S.D. $^{*}p < 0.05$ and $^{\dagger}p < 0.01$ *vs.* donors.

Thus, the trend to decreased spontaneous phosphorylation of pro-survival protein kinase B (Akt1) as compared to normal cells, after UV exposure turned into a statistically significant suppression of phosphorylation activity in AV keratinocytes (Fig. 7A). By contrast, NAV keratinocytes expressed maximal spontaneous and UV-induced levels of phosphorylated p53 (pro-apoptotic protein).

Exposure of normal human keratinocytes to HNE leads to increased H_2O_2 production, upregulation of GSTA1, and downregulation of GSTM1 protein, transient inhibition of Erk1/2 and Akt phosphorylation, overexpression of SOX-2, CAT, GSTM1, bFGF, and IL-6 genes, and NAV-like cytokine protein expression

Exposure of normal keratinocytes to a nontoxic physiological concentration of HNE (25 μM) induced H_2O_2 production by cells. After 4 h, the concentration of H_2O_2 in the conditioned medium reached the levels observed in the cultures of AV and NAV cells (approx. 0.5 nmol/ml, corresponding to 0.5 μM) (Fig. 3). Increased DCF-DA fluorescence in keratinocytes treated with HNE indicated intracellular H_2O_2 overproduction (data not shown). The same exposure led to increased GSTA1 and decreased GSTM1 protein expression, leaving unchanged GSTP1 protein levels (Fig. 5B). The HNE effects on several genes were transient, with maximum observed at 1 h for *GSTM1*, *CAT*, *bFGF*, and *IL-6* and minimum for *MCP1* (Fig. 8A). Upregulation of iNOS and IL-6 and downregulation of IL-8 reached statistical significance at 4 h. Erk1/2 and Akt phosphorylation was significantly and transiently inhibited by HNE at 0.5 and 1 h incubation, with a recovery at 2 h (Fig. 7B). The pattern of cytokines in the conditioned medium at 4 h displayed many features resembling the NAV pattern (Figs. 6A–6C) (*i.e.*, statistically significantly increased levels of IL-6, IL-7, IP-10, PDFGbb, and VEGF in particular). Levels of bFGF, MCP-1, and G-CSF proteins were not affected by the presence of exogenous HNE.

Discussion

In the vast literature dedicated to the vitiligo problem, we failed to find data on impaired redox signaling as a possible molecular basis for the melanocyte loss in vitiligo. Here, we observed rather peculiar generalized redox disturbances, characterized by low catalase and GST activities, low GSH and GSSG levels in erythrocytes, higher than normal HNE–protein adducts in plasma, and normal total release of strong pro-oxidant species from circulating white blood cells, as revealed by the physiological values of LDCL and nitrates/nitrites in vitiligo blood (Fig. 2). This pattern of redox imbalance is different from that repeatedly reported for inflammatory states, where pro-oxidant formation by circulating white blood cells is increased, and antioxidant enzymes are activated/upregulated to neutralize ROS overproduction (6, 21). The inhibition of catalase by millimolar concentrations of its substrate H_2O_2, shown indirectly in the early work of Schallreuter *et al.* (35) and stated repeatedly in the following publications, seems to be unlikely to occur. In fact H_2O_2, even at submillimolar (0.25–0.40 mM) concentrations, already causes erythrocyte destruction and methemoglobin formation in both normal and hemolytic anemia red cells (38). Contrarily, vitiligo patients suffer neither any disturbances

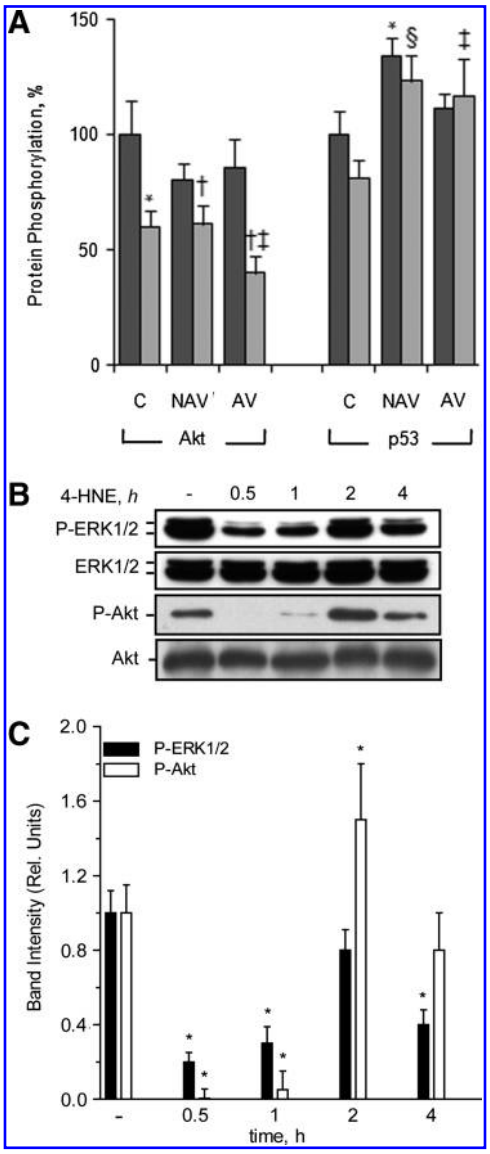

FIG. 7. Spontaneous, UV-, or HNE-induced phosphorylation of Akt1, p53, and Erk1/2 in cultivated human keratinocytes. (**A**) Baseline (*black bars*) and UV-induced (*gray bars*) phosphorylated proteins in the control (**C**), nonaffected (NAV), and affected (AV) keratinocytes. UV-induced phosphorylation was determined 30 min after irradiation. Data are expressed in per cent to the control nonirradiated cells. Statistics is as in Figure 4. (**B**, **C**) Dynamics of Erk1/2 and Akt phosphorylation in the control human keratinocytes exposed to 25 μM of HNE. *$p < 0.05$ *vs.* untreated controls (-).

of erythrocyte stability, nor excessive hemoglobin oxidation. Erythrocyte catalase might exert low activity due to two factors: (a) a genetic basis, due to the *CAT* gene polymorphism, or (b) an epigenetic background when catalase, being specifically targeted by HNE, looses its catalytic activity (14, 23). Several SNPs in the *CAT* gene have been identified, and the heterozygous genotype for T/C SNP in exon 9 was shown to be linked to vitiligo in large groups of patients of different ethnicity (36). However, the association of this *CAT* SNP with the risk of vitiligo, the type of depigmentation, and with catalase activity is still under discussion (14, 29, 47). In accord with a computer simulation, the *CAT* SNP affects the protein stability and enzymatic activity, rendering its active NADPH-binding and tetramerization domains excessively sensitive to oxidation by H_2O_2 (44). As for GST activity, its inhibition could also be due to polymorphic changes in two GST isoforms (GSTM and GSTT), that are characteristic for vitiligo patients (42), and cause partial loss of the total enzyme activity and impaired HNE detoxification (18). Impaired HNE metabolism consequently increases the probability of HNE-protein adduct formation (Fig. 2), followed by the inactivation of HNE-sensitive enzymes such as CAT and GST (11, 14, 23). Of interest, it has been shown that HNE–CAT complexes possess neo auto-antigen properties (23), inducing the consequent autoimmune reaction frequently observed in the patients affected by vitiligo (Table 1) or systemic lupus erythematosus. We could also hypothesise a derangement of the adaptive response to the increased levels of H_2O_2/HNE, due to the inherited vitiligo defect. This may, for example, affect Nrf-2-regulated ARE (antioxidant responsive elements)- or EpRE (electrophile-responsive element)-mediated gene expression of the phase II, antioxidant and glutathione synthesizing enzymes (48), followed by abnormal cytokine production, as it has been shown for the genetically-based cystic fibrosis defect (9). Our data relative to low GSH and GSSG levels in vitiligo erythrocytes (Fig. 2) seem to support this hypothesis as well. In addition, we found distinct changes in the plasma cytokine pattern (Fig. 3), namely lower than normal levels of (i) TNFα, a primary trigger and marker of inflammatory response, (ii) the pro-inflammatory IL-8 chemokine for granulocytes, the overexpression of which is characteristic of skin chronic inflammation (30), and (iii) MCP-1, a chemokine for monocytes highly expressed after skin wounding (33). Although the bactericidal role of H_2O_2 released during inflammation is commonly accepted, the H_2O_2-regulated promotion or inhibition of inflammatory response is still under discussion. Depending on extracellular concentration, H_2O_2 up to 25 μM increases the expression of several pro-inflammatory NFκB-dependent and TNFα-induced genes, such as IL-8, MCP-1, and TNFα, whereas at higher concentrations it exerts an inhibitory effect on these genes in the immune cells (27). Taking into account the low CAT activity in the circulating erythrocytes and white blood cells of vitiligo patients (13, 46), plasma levels of H_2O_2 may remain within the noncytotoxic range (lower than 0.25 mM), nevertheless reaching the anti-inflammatory threshold.

Experiments with suction-blistered vitiligo epidermis or immunohystochemical analysis of vitiligo biopsies have revealed several major differences between affected and nonaffected skin areas, such as cytokine expression and pro-apoptotic behavior in the keratinocytes of the affected zones (24, 26). Cultured vitiligo keratinocytes derived from depigmented skin have lower than normal lifespan, cannot maintain growth of allogeneic melanocytes, and express prevalently pro-apoptotic proteins (5). Keratinocytes expanded from nonaffected vitiligo skin behave in an intermediate mode between control and AV cells. All these differences become evident at the latest passages of keratinocyte cultures, close to their maximum lifespan. On the other hand, at the early passages during adaptation to the culture conditions, AV and control keratinocytes do not show any differences and, in addition, NAV cells are more vital, with lower molecular markers and cellular features of apoptosis than the

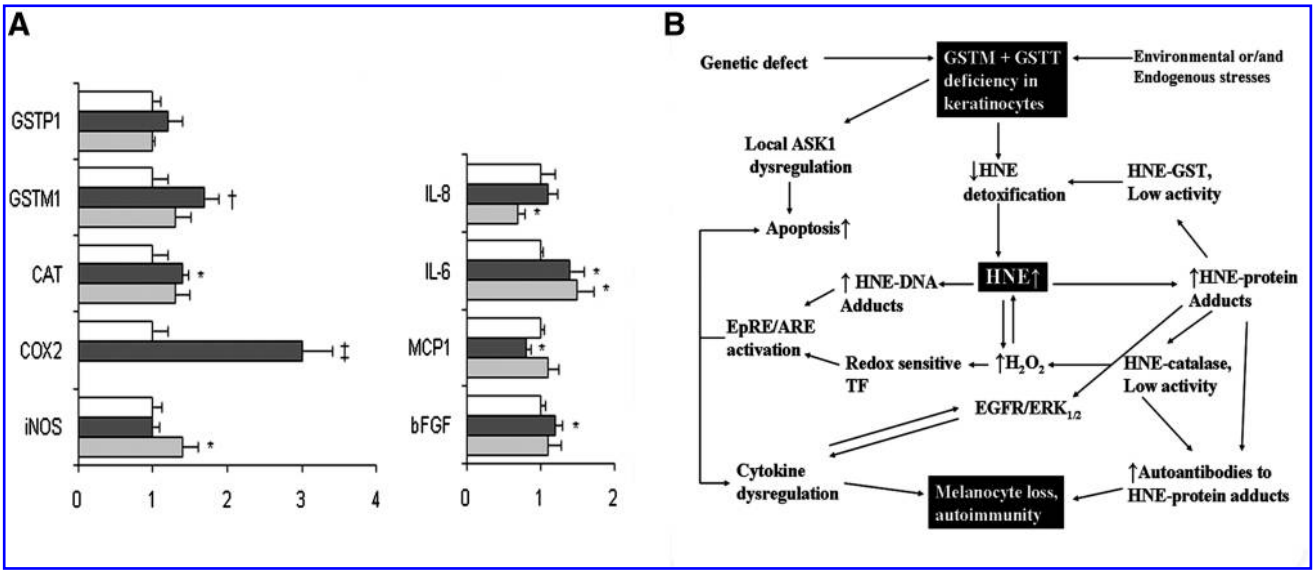

FIG. 8. HNE effects on gene expression in normal human keratinocytes (A) and hypothetical scheme of redox-regulated melanocyte loss in vitiligo (B). (**A**) Keratinocytes were cultivated without HNE (*empty bars*) or with 25 μM HNE for 1 h (*black bars*) and 4 h (*gray bars*). Relative gene expressions are present as mean ± S.D. of three independent experiments on three keratinocyte lines. $^{*}p < 0.05$, $^{\dagger}p < 0.01$, and $^{\ddagger}p < 0.001$ *vs.* untreated keratinocytes. (**B**) GST, HNE, and H_2O_2 interconnections in the hypothetical mechanism of keratinocyte-based redox-regulated melanocyte loss in vitiligo. ASK1, apoptosis-signal-regulating kinase; EpRE and ARE, electrophile and antioxidant regulated elements, respectively; GSTM and GSTT, isoforms mu and theta of glutathione S-transferase, respectively; TF, transcription factors.

control keratinocytes (5). Here, we observed numerous and significant baseline and UV-induced redox/cytokine differences between normal, AV and NAV keratinocytes at their early culture passages, when vitiligo cells did not yet display any apoptotic propensity or inability to maintain melanocytes in co-culture (Figs. 1B and 1C). Of note, the presence of allogeneic melanocytes did not influence any parameter measured in the pure keratinocyte cultures. Both types of vitiligo keratinocytes produced H_2O_2 in much higher quantities than normal cells, although its concentration never exceeded 0.5 μM (Fig. 3B). Similar levels of extracellular H_2O_2 were observed in normal keratinocytes treated by HNE (Fig. 3D), which was in good agreement with the previous literature (41) and with our own data on HNE-induced intracellular H_2O_2 levels in keratinocytes. Notably, HNE has been recognized as an endogenous ligand for EGFR (25), which may result in NOX induction (22) and increased H_2O_2 formation. We found *CAT* gene expression slightly downregulated in AV cells exclusively (Fig. 4A), and we did not find any changes in CAT protein expression in both types of vitiligo cells, in accord with the published data on vitiligo epidermis (36).

For the first time, we detected distinct defects of GST in both types of vitiligo keratinocytes [low GSTM1 and GSTT1 gene expression (Fig. 4A), low GSTM1 protein expression (Fig. 5A), and low GST activity towards HNE (Fig. 3)]. The impaired *CAT*, *GSTM1*, and *GSTT1* gene expression in vitiligo cells (Fig. 4) was left unchanged upon exposure to low-dose solar simulating UV. While chronic UV exposure is clearly involved in a variety of skin pathologies, short-term mild UV irradiation stimulates epidermal cell proliferation and induces the keratinocytes to produce nitric oxide and distinct paracrine melanogenic cytokines, such as bFGF, SCF, and endothelin-1 (39). Correspondingly, we observed that UV did improve spontaneously downregulated iNOS and bFGF genes in AV keratinocytes (Fig. 4). These data seem to support our hypothesis that inherited defects of GSTM1, GSTT1, and, probably, catalase might impair the adaptive cellular response to various stressors, namely H_2O_2, HNE, and mild UV irradiation. Therefore, abnormal levels of H_2O_2 due to HNE-induced formation and to decreased neutralization by defective catalase (13, 36, 43) may shift its regulatory action towards the expression of various cytokines and growth factors controlled through redox signaling, among which are VEGF, PDGF, MCP-1 (33, 37), IL-6, IL-8, and TNFα (22, 27). Not surprisingly, we found a severe dysregulation of these cytokines both in keratinocytes and in the plasma of patients affected by vitiligo (Fig. 6). Moreover, upregulation of VEGF, PDGF, and IP-10 proteins, a characteristic feature of both AV and NAV keratinocytes, was induced in normal keratinocytes by exogenous HNE, probably via a H_2O_2-mediated mechanism. Exposure to noncytotoxic concentrations of HNE led also to the downregulation of IL-8 and MCP-1 genes (Fig. 8A). The same chemokines were suppressed in the vitiligo plasma and AV cells. IL-8 and MCP-1 normally trigger H_2O_2 overproduction in the skin, both by attracting H_2O_2-generating cells such as granulocytes and monocytes (33), and by inducing NOX in nonphagocytozing skin cells through the interaction with EGFR (22). Hence, low expression of these chemokines in vitiligo may play a protective role by limiting H_2O_2 formation in the skin. In general, the perturbed cytokine pattern in vitiligo keratinocytes may be a consequence of the impaired EGFR-mediated and ERK1/2-controlled pathway of cytokine expression (30), induced by HNE.

The defects of GST expression and activity towards HNE in vitiligo keratinocytes result in dysregulated levels of this electrophil (Fig. 3). Normally, HNE at low concentrations regulates stress gene response and apoptosis *via* the AP-1-dependent pathways inhibiting the pro-survival ERK1/2- and

Akt-regulated pathways (34), and *via* the stimulating pro-apoptotic p53 pathway (41). Accordingly, we found an early time-dependent inhibition of ERK1/2 and Akt1 phosphorylation in normal human keratinocytes exposed to HNE (Fig. 7). We also observed inhibited UV-induced Akt1, and enhanced spontaneous+UV-induced p53 phosphorylation in vitiligo keratinocytes, probably caused by endogenous HNE (Fig. 7). Impaired GSTM1 expression/induction may also negatively affect cellular functions, by acting in a nonenzymatic mode, for example, inducing ASK-1-controlled apoptosis normally inhibited by GSTM1 (10), or dysregulating the protein kinase cascade (40).

Collectively, our mechanistic study revealed new pieces in the vitiligo "puzzle" (43), such as GST and HNE which, together with the known ones, namely H_2O_2 and catalase, may well be included in the hypothetic redox-regulated mechanism of melanocyte loss (Fig. 8B), and might represent good candidates as therapeutic targets for this skin disease.

Acknowledgments

This work was supported by The Italian Ministry for Health (Grant IDI IRCCS-2008). The skillful technical assistance of Dr. Emanuel Paionni is gratefully acknowledged.

Author Disclosure Statement

No competing financial interests exist.

References

1. Aebi H. Catalase *in vitro. Methods Enzymol* 105: 121–126, 1984.
2. Alin P, Danielson UH, and Mannervik B. 4-hydroxyalk-2-enals are substrates for glutathione transferase. *FEBS Lett* 179: 267–279, 1985.
3. Bartosz G. Reactive oxygen species: Destroyers or messengers? *Biochem Pharmacol* 77: 1303–1315, 2009.
4. Bolt HM and Their R. Relevance of the deletion polymorphisms of the glutathione S-transferases GSTT1 and GSTM1 in pharmacology and toxicology. *Curr Drug Metab* 7: 613–628, 2006.
5. Bondanza S, Maurelli R, Paterna P, Migliore E, Di Giacomo F, Primavera G, Paionni E, Dellambra E, and Guerra L. Keratinocyte cultures from involved skin in vitiligo patients show an impaired *in vitro* behaviour. *Pigment Cell Res* 20: 288–300, 2007.
6. Brown GE, Silver GM, Reiff J, Allen RC, and Fink MP. Polymorphonuclear neutrophil chemiluminescence in whole blood from blunt trauma patients with multiple injuries. *J Trauma* 46: 297–305, 1999.
7. Casp, CB, She JX, and McCormack, WT. Genetic association of the catalase gene (CAT) with vitiligo susceptibility. *Pigment Cell Res* 15: 62–66, 2002.
8. Cesareo E, Parker LJ, Pedersen JZ, Nuccetelli M, Mazzetti AP, Pastore A, Federici G, Caccuri AM, Ricci G, Adams JJ, Parker MW, and Lo Bello M. Nitrosylation of human glutathione transferase P1-1 with dinitrosyl diglutathionyl iron complex *in vitro* and *in vivo. J Biol Chem* 280: 42172–42180, 2005.
9. Chen J, Kinter M, Shank S, Cotton C, Kelley TJ, and Ziady AG. Dysfunction of Nrf-2 in CF epithelia leads to excess intracellular H2O2 and inflammatory cytokine production. *PLoS One* 3: e3367, 2008.
10. Cho SG, Lee YH, Park HS, Ryoo K, Kang KW, Park J, Eom SJ, Kim MJ, Chang TS, Choi SY, Shim J, Kim Y, Dong MS, Lee MJ, Kim SG, Ichijo H, and Choi EJ. Glutathione S-transferase mu modulates the stress-activated signals by suppressing apoptosis signal-regulating kinase 1. *J Biol Chem* 276: 12749–12755, 2001.
11. Codreanu SG, Zhang B, Sobecki SM, Billheimer DD, and Liebler DC. Global analysis of protein damage by the lipid electrophile 4-hydroxy-2-nonenal. *Mol Cell Proteomics* 8: 670–680, 2009.
12. Dammak I, Boudaya S, Ben Abdullah F, Turki H, Attia H, and Hentati B. Antioxidant enzymes and lipid peroxidation at the tissue level in patients with stable and active vitiligo. *Int J Dermatol* 48: 476–480, 2009.
13. Dell'Anna ML, Urbanelli S, Mastrofrancesco A, Camera E, Iacovelli P, Leone G, Manini P, D'Ischia M, and Picardo M. Alterations of mitochondria in peripheral blood mononuclear cells of vitiligo patients. *Pigment Cell Res* 16: 553–559, 2003.
14. D'souza A, Kurien, BT, Rodgers R, Shenoi J, Kurono S, Matsumoto H, Hensley K, Nath SK, and Scofield RH. Detection of catalase as a major protein target of the lipid peroxidation product 4-HNE and the lack of its genetic association as a risk factor in SLE. *BMC Med Gen* 9: 62, 2008.
15. Fourquet S, Huang ME, D'Autreaux B, and Toledano MB. The dual functions of thiol-based peroxidises in H_2O_2 scavenging and signalling. *Antioxid Redox Signal* 10: 1565–1575, 2008.
16. Guerra L, Primavera G, Raskovic D, Pellegrini G, Golisano O, Bondanza S, Paterna P, Sonego G, Gobello T, Atzori F, Piazza P, Luci A, and De Luca M. Erbium:YAG laser and cultured epidermis in the surgical therapy of stable vitiligo. *Arch Dermatol* 139: 1303–1310, 2003.
17. Habig WH, Pabst MJ, and Jakoby WB. Glutathione S-transferases. The first enzymatic step in mercapturic acid formation. *J Biol Chem* 249: 7130–1739, 1974.
18. Hayes JD, Flanagan JU, and Jowsey IR. Glutathione transferases. *Ann Rev Pharmacol Toxicol* 45: 51–88, 2005.
19. Hiratsuka A, Saito H, Hirose K, and Watabe T. Marked expression of glutathione S-transferase A4-4 detoxifying 4-hydroxy-2(E)-nonenal in the skin of rats irradiated by ultraviolet B-band light (UVB). *Biochem Biophys Res Commun* 260: 740–746, 1999.
20. Imokawa G. Autocrine and paracrine regulation of melanocytes in human skin and in pigmentary disorders. *Pigment Cell Res* 17: 96–110, 2004.
21. Kharaeva Z, Gostova E, De Luca C, Raskovic D, and Korkina L. Clinical and biochemical effects of coenzyme Q_{10}, vitamin E, and selenium supplementation to psoriasis patients. *Nutrition* 25: 295–302, 2009.
22. Korkina L and Pastore S. The role of redox regulation in the normal physiology and inflammatory diseases of the skin. *Front Biosci* 1: 123–141, 2009.
23. Kurien BT, Hensley K, Bachmann M, and Scofield RH. Oxidatively modified autoantigens in autoimmune diseases. *Free Rad Biol Med* 15: 549–556, 2006.
24. Lee AY, Kim NH, Choi WI, and Youm YH. Less keratinocyte-derived factors related to more keratinocyte apoptosis in depigmented than in normally pigmented suction-blistered epidermis may cause passive melanocyte death in vitiligo. *J Invest Dermatol* 124: 976–983, 2005.
25. Liu W, Akhand AA, Kato M, Yokoyama I, Miyata T, Kurokawa K, Uchida K, and Nakashima I. 4-hydroxynonenal triggers an epidermal growth factor-linked signal pathway for growth inhibition. *J Cell Sci* 112: 2409–2417, 1999.
26. Moretti S, Spallanzani A, Amato L, Hautmann G, Gallerani I, Fabiani M, and Fabbri P. New insights into the patho-

genesis of vitiligo: Imbalance of epidermal cytokines at sites of lesions. *Pigment Cell Res* 15: 87–92, 2002.
27. Oliveira–Marques de V, Cyrne L, Marinho HS, and Antunes F. A quantitative study of NF-kappaB activation by H2O2: relevance in inflammation and synergy with TNF-alpha. *J Immunol* 178: 3893–3902, 2007.
28. Paglia DE and Valentine WN. Studies on quantitative and qualitative characterization of erythrocyte glutathione peroxidase. *J Lab Clin Med* 70: 158–169, 1967.
29. Park HH, Ha E, Uhm YK, Jin SY, Kim YJ, Chung JH, and Lee MH. Association study between catalase gene polymorphisms and the susceptibility to vitiligo in Korean population. *Exp Dermatol* 15: 377–380, 2006.
30. Pastore S, Mascia F, Mariotti F, Dattilo C, Mariani V, and Girolomoni G. ERK1/2 regulates epidermal chemokine expression and skin inflammation. *J Immunol* 174: 5047–5056, 2005.
31. Pizzimenti S, Ferracin M, Sabbioni S, Toaldo C, Pettazzoni P, Dianzani MU, Negrini M, and Barrera G. MicroRNA expression changes during human leukemic HL-60 cell differentiation induced by 4-hydroxynonenal, a product of lipid peroxidation. *Free Rad Biol Med* 46: 282–288, 2009.
32. Reed DJ, Babson JR, Beatty PW, Brodie AE, Ellis WW, and Potter DW. High performance liquid chromatography analysis of nanomole levels of glutathione disulphide and related thiols and disulphides. *Anal Biochem* 106: 55–62, 1980.
33. Roy S, Khanna S, Nallu K, Hunt TK, and Sen CK. Dermal wound healing is subject to redox control. *Mol Ther* 13: 211–220, 2006.
34. Sampey BP, Carbone DL, Doorn JA, Drechsel DA, and Petersen DR. 4-hydroxy-2-nonenal adduction of extracellular signal-regulated kinase (Erk) and the inhibition of hepatocyte Erk-Est-like protein-1-activating protein-1 signal transduction. *Mol Pharm* 71: 871–883, 2007.
35. Schallreuter KU, Wood JM, and Berger J. Low catalase levels in the epidermis of patients with vitiligo. *J Invest Dermatol* 97: 1081–1085, 1991.
36. Schallreuter KU, Bahadoran P, Picardo M, Slominski A, Elassiuty YE, Kemp EH, Giachino C, Liu JB, Luiten RM, Lambe T, Le Poole IC, Dammak I, Onay H, Zmijewski MA, Dell'Anna ML, Zeegers MP, Cornall RJ, Paus R, Ortonne JP, and Westerhof W. Vitiligo pathogenesis: Autoimmune disease, genetic defect, excessive reactive oxygen species, calcium imbalance, or what else? *Exp Dermatol* 17: 139–160, 2008.
37. Sen CK, Khanna S, Babior BM, Hunt TK, Ellison EC, and Roy S. Oxidant-induced vascular endothelial growth factor expression in human keratinocytes and cutaneous wound healing. *J Biol Chem* 277: 33284–33290, 2002.
38. Snyder LM, Sauberman N, Condara H, Dolan J, Jacobs J, Szymanski I, and Fortier NL. Red cell membrane response to hydrogen peroxide-sensitivity in hereditary xerocytosis and in other abnormal red cells. *Br J Haematol* 48: 435–444, 1981.
39. Sriwiriyanont P, Ohuchi A, Hachiya A, Visscher MO, and Boissy RE. Interaction between stem cell factor and endothelin-1: Effects on melanogenesis in human skin xenografts. *Lab Invest* 86: 1115–1125, 2006.
40. Townsend DM, Findlay VL, and Tew KD. Glutathione S-transferases as regulators of kinase pathways and anticancer drug targets. *Methods Enzymol* 401: 287–307, 2005.
41. Uchida K, Shiraishi M, Naito Y, Torii Y, Nakamura Y, and Osawa TA. Activation of stress signaling pathways by the end product of lipid peroxidation. *J Biol Chem* 274: 2234–2242, 1999.
42. Uhm YK, Yoon SH, Kang IJ, Chung JH, Yim SV, and Lee MH. Association of glutathione S-transferase gene polymorphisms (GSTM1 and GSTT1) of vitiligo in Korean population. *Life Sci* 81: 223–227, 2007.
43. Westerhof W and D'Ischia M. Vitiligo puzzle: The pieces fall in place. *Pigment Cell Res* 20: 345–359, 2007.
44. Wood JM, Gibbons NC, Chavan B, and Schallreuter KU. Computer simulation of heterogeneous single nucleotide polymorphisms in the catalase gene indicates structural changes in the enzyme active site, NADPH-binding and tetramerization domains: A genetic predisposition for an altered catalase in patients with vitiligo? *Exp Dermatol* 17: 366–371, 2008.
45. Yang Y, Yang Y, Xu Y, Lick SD, Awashti YC, and Boor PJ. Endothelial glutathione-S-transferase A4-4 protects against oxidative stress and modulates iNOS expression through NF-kappa B translocation. *Toxicol Appl Pharmacol* 230: 187–196, 2008.
46. Yildirim M, Baysal V, Inaloz HS, Kesici D, and Delibas N. The role of oxidants and antioxidants in generalized vitiligo. *J Dermatol* 30: 104–108, 2003.
47. Zamocky M, Furtmuller PG, and Obinger C. Evolution of catalases from bacteria to humans. *Antioxid Redox Signal* 10: 1527–1547, 2008.
48. Zhang H and Forman HJ. Signaling pathways involved in phase II gene induction by alpha, beta-unsaturated aldehydes. *Toxicol Ind Health* 25: 269–278, 2009.

Address correspondence to:
Professor Dr. Liudmila Korkina
Laboratory of Tissue Engineering and Cutaneous Pathophysiology
Istituto Dermopatico dell'Immacolata (IDI IRCCS)
Via Monti di Creta 104
Rome 00167
Italy

E-mail: l.korkina@idi.it

Date of first submission to ARS Central, November 2, 2009; date of final revised submission, January 8, 2010; date of acceptance, January 13, 2010.

Abbreviations Used

Akt = protein kinase B
AOA = total antioxidant activity
ARE = antioxidant responsive elements
ASK = apoptosis-signal-regulating kinase
AV = affected vitiligo
bFGF = basic fibroblast growth factor
CAT = catalase
CDNB = 1-chloro-2,4-dinitrobenzene
CL = chemiluminescence
COX = cyclooxygenase
DCF-DA = 2′,7′-dichlorofluorescein diacetate
DMEM = Dulbecco's modified Eagle's medium
EGF = epidermal growth factor
EpRE = electrophile-responsive element
ERK = extracellular regulation kinase
FCS = fetal calf serum
GAPDH = glyceraldehyde 3 phosphate dehydrogenase
G-CSF = granulocyte colony stimulating factor
GM-CSF = granulocyte macrophage colony stimulating factor
GPx = glutathione peroxidase
GSH = reduced glutathione
GSSG = oxidized glutathione
GST = glutathione-S-transferase
HNE = 4-hydroxy-2-nonenal
IFNγ = interferon gamma
IL = interleukin
iNOS = inducible nitric oxide synthase
IP-10 = interferon gamma-produced protein of 10kDa
LDCL = luminol-dependent chemiluminescence
L-DOPA = 3,4 dihydroxyphenylalanine
MCP-1 = monocyte chemotactic protein 1
MDA = malonyl dialdehyde
MIP = macrophage inflammatory protein
NAV = non affected vitiligo
NOX = NADPH oxidase
Nrf-2 = NF-E2 related factor
PBS = phosphate buffer solution
PDGF = platelet-derived growth factor
PMA = phorbol 12-myristate 13-acetate
ROS = reactive oxygen species
SCF = stem cell factor
SDS = sodium dodecyl sulfate
SNP = single nucleotide polymorphism
SOD = superoxide dismutase
TNFα = tumour necrosis factor alpha
VEGF = vascular endothelium growth factor

This article has been cited by:

1. Roberta Colucci, Torello Lotti, Silvia Moretti. 2012. Vitiligo: an update on current pharmacotherapy and future directions. *Expert Opinion on Pharmacotherapy* **13**:13, 1885-1899. [CrossRef]
2. Maria Lucia Dell'Anna, Muriel Cario-André, Barbara Bellei, Alain Taieb, Mauro Picardo. 2012. In vitro research on vitiligo: strategies, principles, methodological options and common pitfalls. *Experimental Dermatology* **21**:7, 490-496. [CrossRef]
3. Yasuhiro Ishihara, Tomohito Kawami, Atsuhiko Ishida, Takeshi Yamazaki. 2012. Tributyltin induces oxidative stress and neuronal injury by inhibiting glutathione S-transferase in rat organotypic hippocampal slice cultures. *Neurochemistry International* **60**:8, 782-790. [CrossRef]
4. D. A. Bassiouny, M. M. Khorshied. 2012. Glutathione S-transferase M1 and T1 genetic polymorphism in Egyptian patients with nonsegmental vitiligo. *Clinical and Experimental Dermatology* no-no. [CrossRef]
5. Fabrizio Guarneri, Alessio Asmundo, Daniela Sapienza, Serafinella P. Cannavò. 2011. Glutathione S-transferase M1/T1 gene polymorphisms and vitiligo in a Mediterranean population. *Pigment Cell & Melanoma Research* no-no. [CrossRef]
6. Liliana Guerra , Desanka Raskovic , Chiara De Luca , Liudmila G. Korkina In Vitro Reconstructed Human Skin Equivalents for Autologous Transplantation in Burns, Chronic Ulcers, and Pigment Defects 62-67. [Abstract] [Full Text PDF] [Full Text PDF with Links]
7. Yasemin G. Isgor, Belgin S. Isgor. 2011. Kinases and glutathione transferases: selective and sensitive targeting. *Frontiers in Biology* **6**:2, 156-169. [CrossRef]
8. Alessandra Pecorelli, Lucia Ciccoli, Cinzia Signorini, Silvia Leoncini, Anna Giardini, Maurizio D'Esposito, Stefania Filosa, Joussef Hayek, Claudio De Felice, Giuseppe Valacchi. 2011. Increased levels of 4HNE-protein plasma adducts in Rett syndrome. *Clinical Biochemistry* **44**:5-6, 368-371. [CrossRef]
9. Nanja van Geel, Reinhart Speeckaert, Alain Taieb, Mauro Picardo, Markus Böhm, David J. Gawkrodger, Karin Schallreuter, Dorothy.C. Bennett, Wietze van der Veen, Maxine Whitton, Silvia Moretti, Wiete Westerhof, Khaled Ezzedine, Yvon Gauthier. 2011. Koebner's Phenomenon in Vitiligo: European Position Paper. *Pigment Cell & Melanoma Research* no-no. [CrossRef]
10. Chiara De Luca, Maria G. Scordo, Eleonora Cesareo, Saveria Pastore, Serena Mariani, Gianluca Maiani, Andrea Stancato, Beatrice Loreti, Giuseppe Valacchi, Carla Lubrano, Desanka Raskovic, Luigia De Padova, Giuseppe Genovesi, Liudmila G. Korkina. 2010. Biological definition of multiple chemical sensitivity from redox state and cytokine profiling and not from polymorphisms of xenobiotic-metabolizing enzymes. *Toxicology and Applied Pharmacology* **248**:3, 285-292. [CrossRef]